Conformational Changes of Bacteriorhodopsin along the Proton-Conduction Chain as Studied with ^{13}C NMR of [3-^{13}C]Ala-Labeled Protein: Arg^{82} May Function as an Information Mediator

Michikazu Tanio,* Satoru Tuzi,* Satoru Yamaguchi,* Ruriko Kawaminami,* Akira Naito,* Richard Needleman,# Janos K. Lanyi,§ and Hazime Saitô*

*Department of Life Science, Himeji Institute of Technology, Harima Science Garden City, Kuoto 3-chome, Kamigori, Hyogo, 678-1297, Japan; #Department of Biochemistry, Wayne State University, Detroit, Michigan 48201 USA; and §Department of Physiology and Biophysics, University of California, Irvine, California 92697-4560 USA

ABSTRACT We have recorded ^{13}C NMR spectra of [3-^{13}C]Ala-labeled wild-type bacteriorhodopsin (bR) and its mutants at Arg^{82}, Asp^{85}, Glu^{194}, and Glu^{204} along the extracellular proton transfer chain. The upfield and downfield displacements of the single carbon signals of Ala^{196} (in the F-G loop) and Ala^{126} (at the extracellular end of helix D), respectively, revealed conformational differences in E194D, E194Q, and E204Q from the wild type. The same kind of conformational change at Ala^{126} was noted also in the Y83F mutant, which lacks the van der Waals contact between Tyr^{83} and Ala^{126} present in the wild type. The absence of a negative charge at Asp^{85} in the site-directed mutant D85N induced global conformational changes, as manifested in displacements or suppression of peaks from the transmembrane helices, cytoplasmic loops, etc., as well as the local changes at Ala^{126} and Ala^{196} seen in the other mutants. Unexpectedly, no conformational change at Ala^{126} was observed in R82Q (even though Asp^{85} is protonated at pH 6) or in D85N/R82Q. The changes induced in the Ala^{126} signal when Asp^{85} is uncharged could be interpreted therefore in terms of displacement of the positive charge of Arg^{82} toward Tyr^{83}, where Ala^{126} is located. It is possible that disruption of the proton transfer chain after protonation of Asp^{85} in the photocycle could cause the same kind of conformational change we detect at Ala^{196} and Ala^{126}. If so, the latter change would be also the result of rearrangement of the side chain of Arg^{82}.

INTRODUCTION

Bacteriorhodopsin (bR) of the archaeon *Halobacterium salinarium* functions as a light-driven proton pump, dependent on photoisomerization of retinal covalently linked to Lys^{216} through a protonated Schiff base (Stoeckenius and Bogomolni, 1982; Mathies et al., 1991; Lanyi, 1993). Its 3D structure is now available at various resolutions from cryo-electron microscopy (Henderson et al., 1990; Grigorieff et al., 1996; Kimura et al., 1997) and x-ray diffraction (Pebay-Peyroula et al., 1997; Luecke et al., 1998; Essen et al., 1998). In the transport cycle a proton is translocated, after absorption of a photon, from the cytoplasmic to the extracellular side of the membrane. This process is initiated by proton transfer from the protonated Schiff base to the anionic Asp^{85}, in the L-to-M reaction (Braiman et al., 1988). The pK_as of Asp^{85} and the proton release group (XH) are strongly dependent on one another, even in unphotolyzed bR (Brown et al., 1995; Govindjee et al., 1996; Richter et al., 1996; Balashov et al., 1997; Althaus and Stockburger, 1998). Glu^{204} and Glu^{194} near the extracellular surface are important residues for normal proton pump activity, because replacement of these residues with glutamine or cysteine abolished both pK_a coupling in the unphotolyzed protein and proton release upon protonation of Asp^{85} in the photocycle (Brown et al., 1995; Govindjee et al., 1996; Balashov et al., 1997; Dioumaev et al., 1998). Room-temperature time-resolved Fourier transform infrared studies have suggested that the proton released might be a delocalized proton in a hydrogen-bonded network between the Schiff base and the extracellular surface and does not originate from Glu^{204} (Rammelsberg et al., 1998). A photovoltage study also indicated that Glu^{204} is not the terminal proton release group (Kalaidzidis et al., 1998). Recently, Luecke et al. (1998) suggested from the structure that a water molecule between Arg^{82} and Glu^{204} may be the origin of the released proton. On the other hand, according to Essen et al. (1998), the terminal proton release complex could be the Glu^{194}/Glu^{204} dyad, which would function as a diffuse proton buffer.

The fact that protonation of Asp^{85} induces the release of a proton from this site indicates that the information of the protonation of Asp^{85} is transmitted to the extracellular surface. Arg^{82}, located between Asp^{85} and the surface, plays an essential role in this because pK_a coupling and proton release in the photocycle are both abolished in R82Q (Govindjee et al., 1996). Molecular dynamics simulations suggest that Arg^{82} reorients toward Glu^{204} in the photocycle (Scharnagl et al., 1995). This mechanism would imply that there is a chain of interacting residues between Asp^{85} and the extracellular surface involving Arg^{82}, Glu^{194} and Glu^{204}, as proposed by Dioumaev et al. (1998) and consistent with the crystallographic structure (Luecke et al., 1998). Protonation of Asp^{85} in the photocycle would perturb the inter-

Received for publication 5 April 1999 and in final form 26 May 1999.

Address reprint requests to Dr. Hazime Saitô, Department of Life Science, Himeji Institute of Technology, Harima Science Garden City, Kuoto 3-chome, Kamigori, Hyogo 678-1297, Japan. Tel: +81-7915-8-0181; Fax: +81-7915-8-0182; E-mail: saito@sci.himeji-tech.ac.jp.

0006-3495/99/09/1577/08 $2.00

actions along the chain and result in a conformational change. It is possible that this sort of conformational change could also be observed in the unphotolyzed state when the residues in this region are altered by mutation. This is the rationale for the work we report here.

In our previous paper (Tanio et al., 1999), we demonstrated with [1-^{13}C]Val-labeled bR that there is conformational coupling of Asp^{85} with distant regions of the protein, either at the cytoplasmic region or near the extracellular surface. This conclusion was based on observations of displacements of ^{13}C NMR chemical shifts in [^{13}C]-labeled bR, which provide an excellent means of probing changes in conformation and dynamics at ambient temperature (Tuzi et al., 1993, 1994, 1996a,b, 1999; Yamaguchi et al., 1998; Tanio et al., 1998). These changes were calibrated by conformation-dependent chemical shifts in model polypeptides, because the ^{13}C chemical shifts of amino acid residues vary very sensitively with their local conformations (up to 8 ppm) (Saitô, 1986; Saitô and Ando, 1989; Saitô et al., 1998). Such an approach proved to be especially useful for revealing the local conformations and dynamics of residues at loops or protruding N- or C-terminal tails (Tuzi et al., 1993, 1994, 1996a,b, 1999; Yamaguchi et al., 1998; Tanio et al., 1998) in membrane proteins. The chemical shifts also served as intrinsic probes for movements of the transmembrane helices. It must be emphasized that the time scale of any conformational fluctuation can easily be distinguished by recording both ^{13}C cross-polarization magic angle spinning (CP-MAS) and dipolar decoupled-magic angle spinning (DD-MAS) NMR spectra. Fast isotropic or large-amplitude ($\tau < 10^{-8}$ s) fluctuations, if any, result in the peak suppression of the former, because of insufficient cross-polarization (Mehring, 1983). Slow anisotropic ($\tau \approx 10^{-5}$ s) fluctuation, if any, suppresses the ^{13}C signals from both measurements, because of interference also with proton decoupling frequency (Rothwell and Waugh, 1981).

In this paper, we show evidence from [3-^{13}C]Ala-labeled bR for the existence of a chain of interacting residues of the extracellular region of the proton channel, using high-resolution ^{13}C solid-state NMR. Our data indicate that the information of the protonation of Asp^{85} is transmitted to the extracellular surface, where Glu^{194} and Glu^{204} are located, and results in conformational changes that may be related to those that induce the release of proton in the photocycle. As for proton release, Arg^{82} plays a key role in the conformational change detected by NMR, because in R82Q the information of the charge state of residue 85 is not transmitted to the region of Ala^{126}.

MATERIALS AND METHODS

L-[3-^{13}C]Alanine was purchased from CIL and used without further purification. *H. salinarium* S9 (wild-type) and its mutants, R82Q, Y83F, D85N, E194Q, E194D, E204Q, and R82Q/D85N, were grown in the TS medium described by Onishi et al. (1965), in which unlabeled L-alanine has been replaced by [3-^{13}C]Ala. Purple or blue membranes from these sources were isolated by a standard method (Oesterhelt and Stoeckenius, 1974). The samples were finally resuspended in 5 mM HEPES buffer containing 10 mM NaCl and 0.025% (w/v) NaN_3 at pH 6 or 7. The preparation of samples at low pH was by the addition of concentrated HCl solution to the samples, which were resuspended twice in distilled water and then briefly sonicated. The pelleted bR preparations were placed in a 5-mm o.d. zirconia pencil-type rotor for NMR measurements. The Teflon cap was glued tightly to the rotor with rapid Alardyte to prevent leakage of water from the samples during magic angle spinning for NMR measurements. Absorption spectra were measured on a Shimadzu UV 2200 UV/visible spectrophotometer.

High-resolution ^{13}C NMR spectra (100.6 MHz) were recorded in the dark at 20°C on a Chemagnetics CMX-400 NMR spectrometer, both by cross-polarization magic angle spinning (CP-MAS) and dipolar decoupled magic angle spinning (DD-MAS) methods, to distinguish the time scale for conformational fluctuation. The spectral width and contact (for CP-MAS), repetition, and acquisition times were 40 kHz, 1 ms, 4 s, and 50 ms, respectively. The $\pi/2$ pulses for carbon and proton nuclei were 5 μs, and the spinning rate was 2.6 kHz. Free induction decays were acquired with data points of 2 K, and Fourier transforms were carried out as 16 K points after 14 K points were zero-filled. ^{13}C chemical shifts were first referred to the carboxyl signal of glycine (176.03 ppm from tetramethylsilane, TMS) and then converted to the relative shifts from the value of TMS.

RESULTS

First, we recorded ^{13}C NMR spectra of [3-^{13}C]Ala-labeled bR and its mutants, to gain insight into the expected conformational changes from disruption of the inter-side-chain hydrogen bonds evident from cryoelectron microscopy and x-ray diffraction (Grigorieff et al., 1996; Pebay-Peyroula et al., 1997; Kimura et al., 1997; Luecke et al., 1998; Essen et al., 1998). Fig. 1 illustrates the ^{13}C CP-MAS (*left*) and DD-MAS (*right*) NMR spectra of the [3-^{13}C]Ala-labeled mutants, E194Q (*B*), E194D (*C*), and E204Q (*D*), as compared with those of wild type (*A*). The assignments (Yamaguchi et al., manuscript in preparation), based on site-directed mutants (Tuzi et al., 1996b, 1999) or partially cleaved proteins, using papain (Tuzi et al., 1994, 1996b) or pronase, are shown at the top of individual peaks, with tentative assignments (including the ones in this paper) in parentheses. The most notable changes associated with the site-specific mutations are at 17.78 ppm (Ala^{196}) and 15.39 ppm (Ala^{126}) in both CP-MAS and DD-MAS NMR spectra (Tuzi et al., 1999). The Ala^{196} signal is displaced upfield to the arrowed peak by 0.61 ppm, depending upon the type of mutation, and the Ala^{126} signal is displaced downfield. In addition, it is noteworthy that the peak intensities of Ala$^{84/240}$ at 16.88 ppm (manuscript in preparation) and 16.19 ppm are significantly decreased in both the CP- and DD-MAS spectra among all of the mutants studied, although the former change cannot be distinguished in the DD-MAS spectrum.

In Fig. 2, the ^{13}C CP-MAS (*left*) and DD-MAS (*right*) NMR spectra of [3-^{13}C]Ala-labeled Y83F were compared with those of wild type (*dotted spectra*). The following changes were noted in the CP-MAS NMR spectra (Fig. 2 *A*): 1) both Ala^{196} and Ala^{126} peaks are either displaced or suppressed; 2) the Ala^{160} or Ala^{103} peak at the cytoplasmic side at 17.13 ppm (Yamaguchi et al., manuscript in preparation) is displaced upfield by 0.07 ppm and the intensity of the peak at 16.19 ppm is decreased, whereas the peak

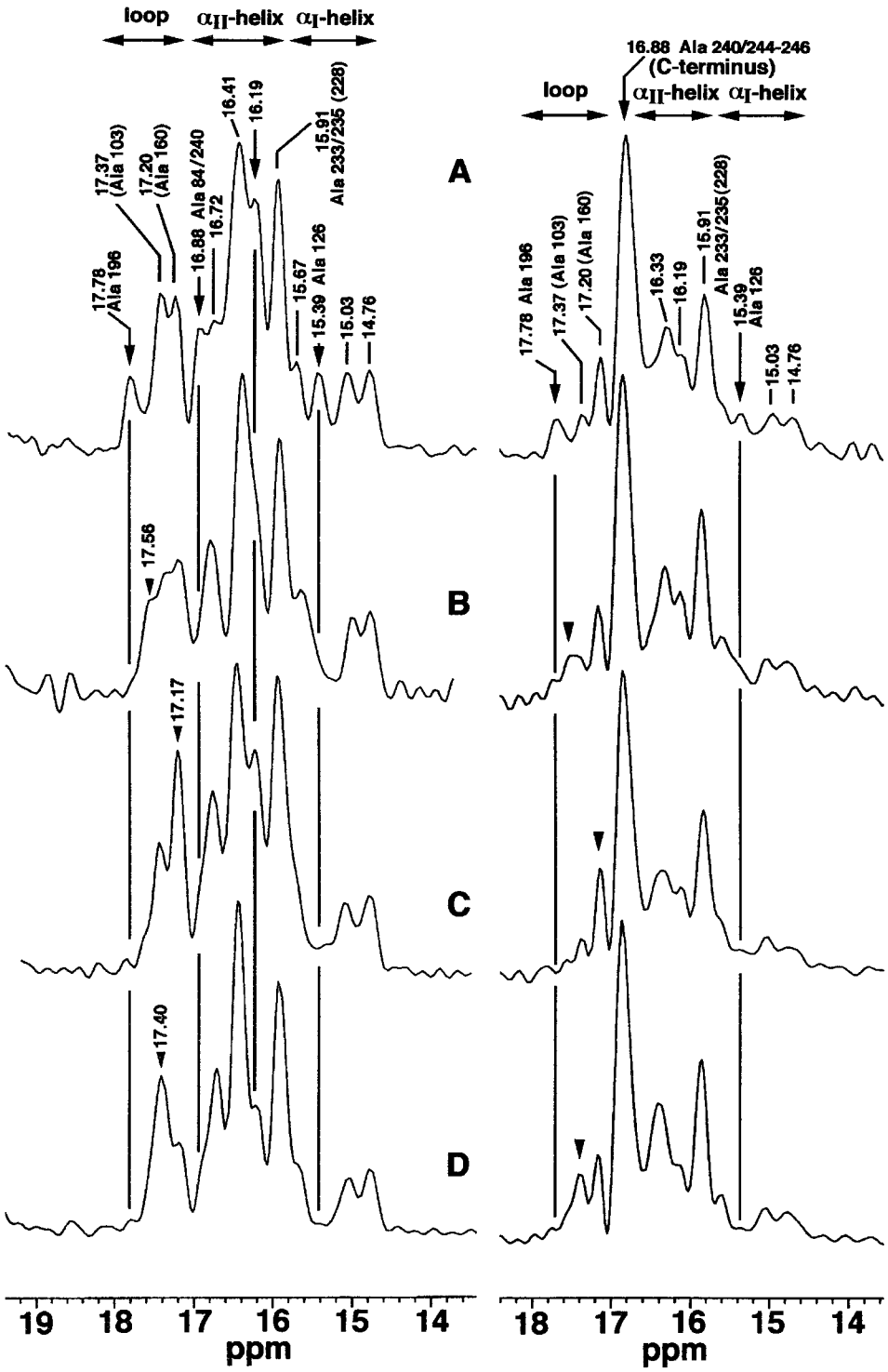

FIGURE 1 100.6 MHz ^{13}C CP-MAS (*left*) and DD-MAS (*right*) NMR spectra of [3-^{13}C]Ala-labeled wild-type bR (*A*), E194Q (*B*), E194D (*C*), and E204Q (*D*) at pH 7. Assigned signals for the wild type, so far completed, are given at the respective peaks, including tentative ones (*parentheses*), as discussed in this paper. The displaced peak positions for Ala^{196} for a variety of the site-directed mutants are indicated by the wedges.

intensity of Ala$^{84/240}$ at 16.88 ppm is substantially enhanced, and 3) the most intense peak at 16.33 ppm is displaced upfield by 0.08 ppm. Because the Ala^{196} peak is clearly visible in the DD-MAS NMR spectrum, we conclude that the peak suppression in the CP-MAS NMR spectrum arose from fast isotropic or large-amplitude fluctuation (with correlation time $< 10^{-8}$ s) (Mehring, 1983). Unexpectedly, the absence of the phenolic hydroxyl group in Tyr^{83} results in conformational fluctuation of Ala^{196} rather than conformational change, in contrast to the cases of E194Q and E194D. This means that the interaction between Glu^{194} and Tyr^{83} may be weaker than expected from the 3D structures (Pebay-Peyroula et al., 1997; Luecke et al., 1998; Essen et al., 1998). On the other hand, the blue-shifted absorption maximum of Y83F (547 nm) indicates that the mutation affects the retinal chromophore.

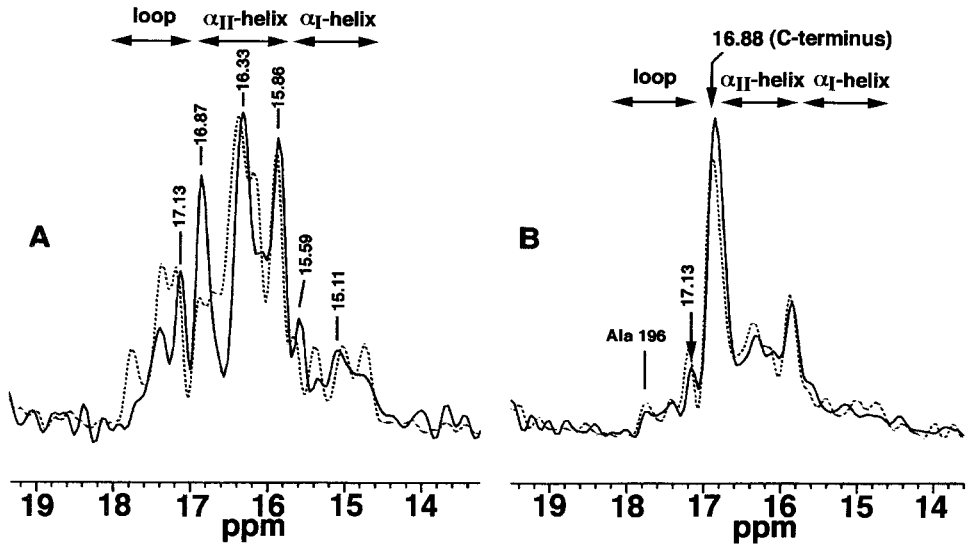

FIGURE 2 100.6 MHz ^{13}C CP-MAS (*A*) and DD-MAS (*B*) NMR spectra of [3-^{13}C]Ala-labeled Y83F mutant at neutral pH. For comparison, the corresponding spectra for the wild type are shown by dotted lines. Indicated peak positions are for the mutant peaks.

More drastic conformational changes were noted in the ^{13}C CP-MAS (*left*) and DD-MAS (*right*) NMR spectra of [3-^{13}C]Ala-labeled D85N (λ_{max} = 605 nm) at pH 7 (Fig. 3), as compared with those of the wild type at pH 7 (λ_{max} = 568 nm) (*dotted spectra*). This indicates that replacement of Asp^{85} with Asn induces drastic global conformational changes that include the transmembrane helices, the extracellular surface, and the cytoplasmic loops, even though from the projection map at 7-Å resolution (Kataoka et al., 1993) the structure of D85N at neutral pH appeared to be very similar to the wild type. In particular, it is noteworthy that the peaks of the transmembrane α_{II}-helices at 16.41 and 16.19 ppm (Tuzi et al., 1994, 1996b) are appreciably suppressed in both CP-MAS and DD-MAS NMR relative to the wild type. This means that these transmembrane helices undergo low-frequency fluctuation in D85N, on a time scale of 10^{-5} s (Rothwell and Waugh, 1981). The Ala^{160} or Ala^{103} and Ala^{84} signals of D85N are displaced upfield by 0.18 and 0.26 ppm, respectively, as compared with those of the wild type, reflecting conformational change at these locations also. Furthermore, the Ala^{196} signal at 17.78 ppm in the wild type is displaced upfield to 17.59 ppm in D85N, whereas Ala^{126} is displaced downfield.

To decide whether these dramatic spectral changes in D85N are caused by the replacement of the aspartate side chain or by the absence of the negative charge at residue 85, we compared the ^{13}C CP-MAS (*left*) and DD-MAS NMR (*right*) spectrum of D85N with those of wild type (*dotted lines*) at low pH (Tuzi et al., 1999) to protonate most of the acidic residues, including Asp^{85} in the wild type (Fig. 4). If the protonated Asp^{85} in the "blue membrane" of the wild-type protein is not equivalent to Asn^{85}, the NMR spectra will be different. The results indicate that this is not so: loss of the charge of residue 85, from protonation in the wild type and from the residue change in the mutant, is responsible for the conformational changes in Fig. 3. At low pH

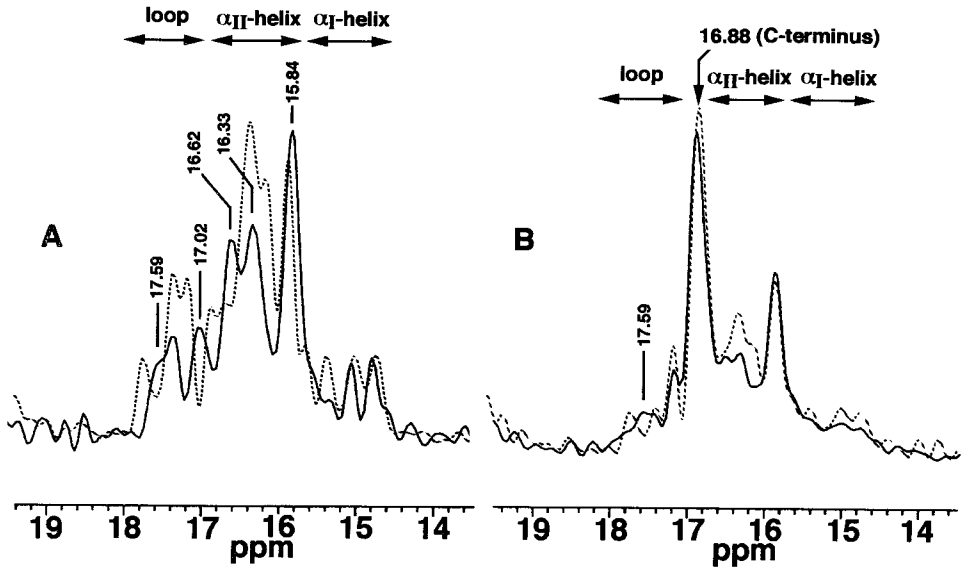

FIGURE 3 100.6 MHz ^{13}C CP-MAS (*A*) and DD-MAS (*B*) NMR spectra of [3-^{13}C]Ala-labeled D85N at pH 7. The dotted spectra are from the wild type at pH 7, for comparison.

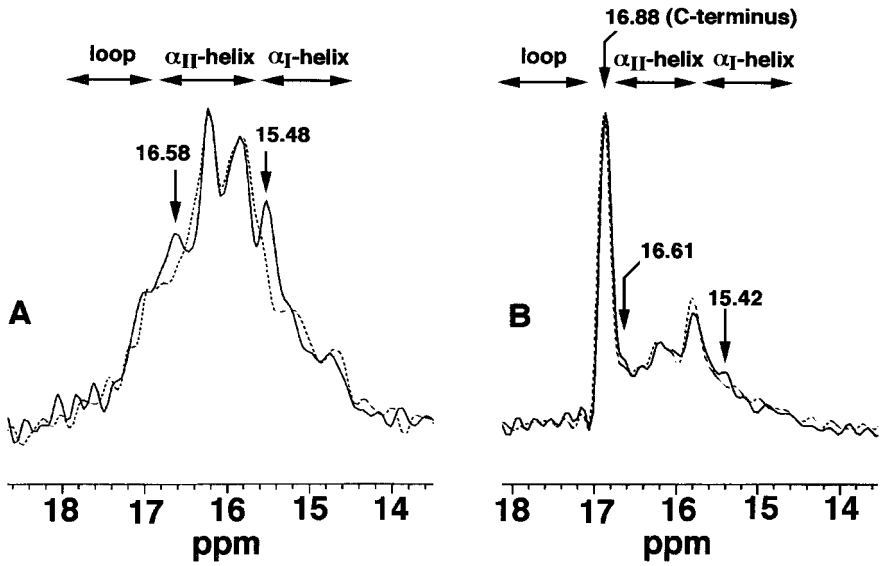

FIGURE 4 100.6 MHz ^{13}C CP-MAS (*A*) and DD-MAS (*B*) NMR spectra of [3-^{13}C]Ala-labeled D85N (——) and wild type (·····) at pH 2.6 and 1.2, respectively.

only the presence or absence of the peaks at ~15.4 and ~16.6 ppm is different between D85N and the wild type. The new peaks at 15.4 and 16.6 ppm could be assigned to a conformational shift of the α-helix, probably from the difference in the side chains of Asp and Asn.

Fig. 5 shows ^{13}C CP-MAS (*left*) and DD-MAS NMR (*right*) spectra of [3-^{13}C]Ala-labeled R82Q (*A*) at pH 6 (λ_{max} = 585 nm) and R82Q/D85N (*B*) (λ_{max} = 581 nm) at pH 7 (the *dotted lines* represent the wild type at pH 7). Under the conditions used (10 mM NaCl), Asp^{85} in R82Q is nearly fully protonated, as indicated by the shift in the absorption maximum with a pK_a (for Asp^{85}) = 7.8 (data not shown). The resulting spectral changes in both mutants are very similar to those in D85N (Fig. 3). The displaced Ala^{196} signal, to 17.53 or 17.57 ppm, in these mutants, as in D85N, indicates that the side chain of Arg^{82} does not influence the

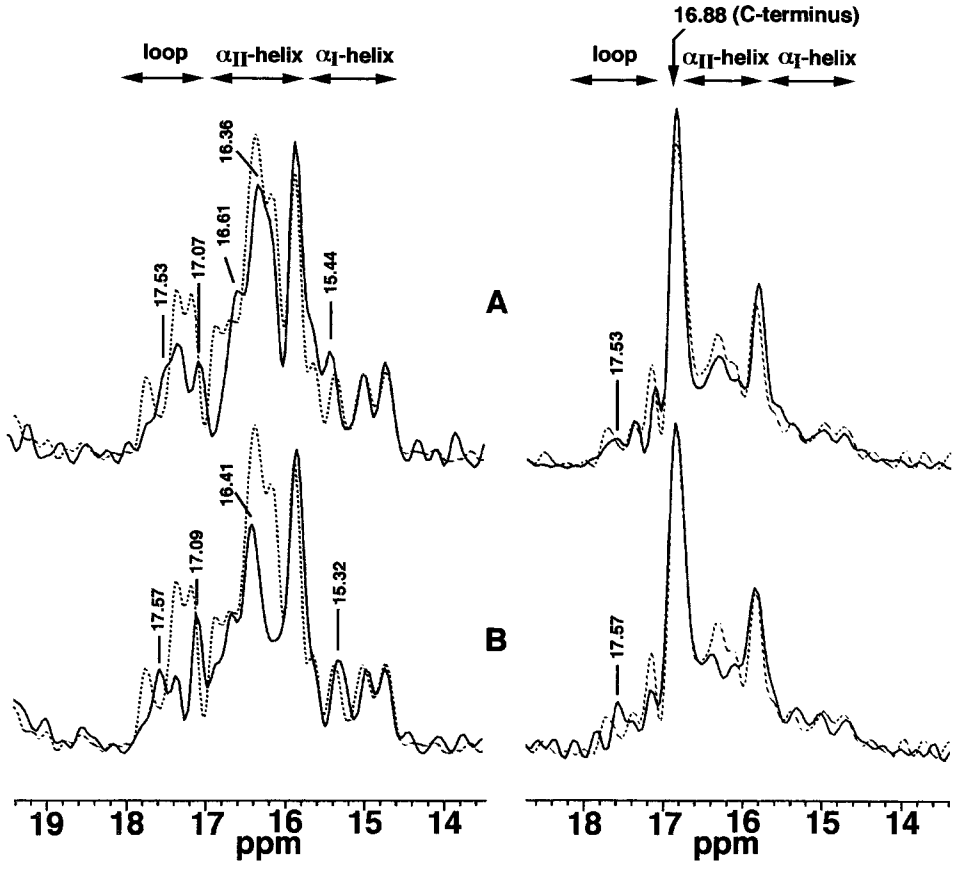

FIGURE 5 100.6 MHz ^{13}C CP-MAS (*left*) and DD-MAS (*right*) NMR spectra of [3-^{13}C]Ala-labeled R82Q (*A*; pH 6) and R82Q/D85N (*B*; pH 7). The dotted spectra are for the wild type at pH 7, for comparison.

effect of Asp^{85} on the local conformation of Ala^{196}. On the other hand, unexpectedly, no spectral change was observed for Ala^{126} in the two R82Q mutants, despite the protonation (in R82Q) or the replacement (in R82Q/D85N) of Asp^{85}. These results imply that the local conformational change at Ala^{126} induced by the absence of negative charge at residue 85 requires the presence of Arg^{82}.

Neither the Ala^{126} nor the Ala^{196} signal was changed in R82Q at pH 8 (λ_{max} = 568 nm) (data not shown). Because at this pH Asp^{85} is about half-deprotonated, the conformation of Ala^{196} must be linked not to Asp^{85} but to the residue change at Arg^{82}. It appears, therefore, that Ala^{196} senses any changes along the hydrogen-bonded chain between Asp^{85} and the extracellular surface. This is unlike the situation with Ala^{126}. The same results indicate that its conformation does not respond to either the protonation or the dissociation of Asp^{85} without the positive charge of Arg^{82}.

DISCUSSION

^{13}C chemical shifts as a probe for conformational change

In our previous papers, we demonstrated that because ^{13}C chemical shifts of particular amino acid residues in [3-^{13}C]Ala- or [1-^{13}C]Val-labeled bR and its site-directed mutants are significantly displaced by changes in the pH or ions and by site-directed mutagenesis, they can be utilized as a convenient probes for detecting conformational changes (Tuzi et al., 1993, 1996b, 1999; Yamaguchi et al., 1998). ^{13}C chemical shifts of the backbone C_α and carbonyl and side-chain C_β signals of a variety of amino acid residues in polypeptides and proteins are generally displaced (up to 8 ppm), depending on their particular conformations, irrespective of the neighboring amino acid residues (Saitô, 1986; Saitô and Ando, 1989; Saitô et al., 1998). The ^{13}C chemical shifts of α-helix, for instance, are displaced in membrane proteins such as bR from those of the reference data, and we suggested that the reason for this is that the conformations of particular residues could be statically or dynamically distorted to form α_{II}-helices (Saitô et al., 1998).

We had demonstrated that the well-resolved single ^{13}C NMR peaks from Ala^{196} in the F-G loop and Ala^{126} at the extracellular turn of helix D locate conformational changes that originate from binding of divalent cations at the extracellular surface (Tuzi et al., 1999). Interestingly, we now find that site-directed mutagenesis at Glu^{204} or Glu^{194} causes similar kinds of spectral changes of the Ala^{196} and Ala^{126} signals (Fig. 1). It appears that mutation at Glu^{204} and Glu^{194} results in conformational change at the F-G loop, including fluctuation of Ala^{196} toward the peak position of random coil (16.88 ppm). As expected, no spectral change at the cytoplasmic loops was induced in these mutants, and the peak positions of characteristic peaks for this loop (Ala^{103} and Ala^{160}) are unchanged (Fig. 1).

The phenolic OH of Tyr^{83} is at van der Waals contact distance from the C_β carbon of Ala^{126} (Grigorieff et al., 1996; Luecke et al., 1998; Essen et al., 1998). The presence or absence of this kind of interaction can be examined in the [3-^{13}C]Ala-Y83F mutant, in which phenolic OH is absent (Fig. 2). The downfield displacement of Ala^{126} signal in the mutant as compared with wild type is consistent with the presence of this sort of interaction. Furthermore, Ala^{196} acquired a conformational fluctuation of time scale of 10^{-9} s, because its CP-MAS NMR signal is suppressed.

Interaction between Asp^{85} and the extracellular surface

Drastic conformational changes are induced for wide areas, including extracellular and cytoplasmic loops and transmembrane helices in R82Q, Y83F, D85N, and R82Q/D85N (Figs. 2, 3, and 5). Undoubtedly, the conformational changes in D85N at pH 7 are caused by the absence of negative charge at Asp^{85}, because the conformation of D85N and wild type is almost the same at low pH (Fig. 4). The observation that protonation of Asp^{85} induces conformational change at the extracellular surface, even when it occurs at neutral pH (Fig. 3), is consistent with our previous data based on [1-^{13}C]Val-labeled protein (Tanio et al., 1999). Significantly, the Ala^{196} signal, from the F-G loop, is displaced in the same way in all of the mutants studied, i.e., in R82Q, D85N, E194D, E194Q, and E204Q. This implicates Arg^{82}, Asp^{85}, Glu^{194}, and Glu^{204} in an interacting chain, in which alterations at any point are communicated to the extracellular surface and produce the same effect. Therefore, we propose here that the conformational changes in Ala^{196} are caused by any sort of modifications at this interacting chain. For the Ala^{196} signal in the Y83F mutants, conformational fluctuation leading to reduced efficiency of cross-polarization is dominant. This also happens for the F-G loop in the D85N at higher pH, which mimics the M state (Kawase et al., manuscript to be published).

We find that the Ala^{126} and Ala^{196} signals are not equally perturbed by a change in the charge of Asp^{85}. The Ala^{126} signal is like the wild type in R82Q at pH 6 and R82Q/D85N at pH 7, even though residue 85 is nearly fully protonated in the former and completely lacks a negative charge in the latter. It has been pointed out that the presence of positive charge at Arg^{82} is required for proton release when Asp^{85} becomes protonated in the photocycle, because the normal order of proton release before uptake is achieved in R82K (Balashov et al., 1995) but not in R82Q (Govindjee et al., 1996). The requirement of Arg^{82} for the conformational change in Ala^{126} in D85N (Fig. 3) may also indicate an effect of the positive charge at Arg^{82}. The crystallographic structure (Luecke et al., 1998) indicates that a diffuse hydrogen-bonded network of polar residues and bound water in the extracellular half-channel serves as the counterion to the positively charged Schiff base, as suggested earlier (de Groot et al., 1989; Dér et al., 1991). If the

information of the protonation state of Asp^{85} is transduced to Glu^{204} and Glu^{194} through this hydrogen-bonding network (Luecke et al., 1998), the conformational changes we detect with ^{13}C NMR at the extracellular surface are probably related to the proton release.

A possible role for Arg^{82} as an information mediator

The results therefore suggest that Arg^{82} is utilized as an information mediator that transmits the effect of the protonation state at Asp^{85} to the Ala^{126} region at the extracellular surface. In what way could Arg^{82} accomplish this? The C_β of Ala^{126} is in van der Waals contact with OH of Tyr^{83}, and its C_α is in van der Waals contact with the indole ring of Trp^{189} (Grigorieff et al., 1996; Luecke et al., 1998; Essen et al., 1998). Indeed, conformational change was noted for Ala^{126} in Y83F also, a mutant in which the hydrogen bond between the OH of Tyr^{83} and the indole N of Trp^{189} cannot form. Although Ala^{126} exhibits this conformational change in the Glu^{194}, Glu^{204}, and D85N mutants, this cannot be induced by direct interaction because the residues are far from being in contact. Instead, all effects from these mutations must be through Tyr^{83} and Trp^{189}. This could be made possible by displacement of the side chain of Arg^{82} toward Tyr^{83}, as manifested from the displacement of the Ala^{126} signal (Figs. 3 and 5) in mutants of Asp^{85}, Glu^{194}, and Glu^{204}, but not in mutants of Arg^{82}.

Because Tyr^{83} is close to Glu^{194} (Pebay-Peyroula et al., 1997; Luecke et al., 1998; Essen et al., 1998), the negative charge of Glu^{194} may facilitate attraction of the side chain of Arg^{82} in the direction of the surface. Recently a ^{15}N NMR study of guanidyl-^{15}N-labeled bR suggested that the side chain of Arg^{82} interacts with an anionic group, presumably with a carboxyl, in M intermediate and D85N (Petkova et al., 1999). Molecular dynamics simulation by Scharnagl et al. (1995), although not by Schulten et al. (Xu et al., 1995; Zhou et al., 1993), suggested that Arg^{82} is reoriented in the M intermediate. We propose that Arg^{82} perturbs the side chain of Tyr^{83} in the photocycle, as implied from the study of mutants in this report. The conformational change around Ala^{126} induced by this interaction may facilitate proton release.

This work has been supported in part by Grants-in-Aid for Scientific Research (B) (09480179 and 09558094) and a Grant-in-Aid for International Scientific Research (Joint Research) (10044092) from the Ministry of Education, Science, Sports and Culture of Japan.

REFERENCES

Althaus, T., and M. Stockburger. 1998. Time and pH dependence of the L-to-M transition in the photocycle of bacteriorhodopsin and its correlation with proton release. *Biochemistry.* 37:2807–2817.

Balashov, S. P., R. Govindjee, E. S. Imasheva, S. Misra, T. G. Ebrey, Y. Feng, R. K. Crouch, and D. R. Menick. 1995. The two pK_a's of aspartate-85 and control of thermal isomerization and proton release in the arginine-82 to lysine mutant of bacteriorhodopsin. *Biochemistry.* 34:8820–8834.

Balashov, S. P., E. S. Imasheva, T. G. Ebrey, N. Chen, D. R. Menick, and R. K. Crouch. 1997. Glutamate-194 to cysteine mutation inhibits fast light-induced proton release in bacteriorhodopsin. *Biochemistry.* 36: 8671–8676.

Braiman, M. S., T. Mogi, T. Marti, L. J. Stern, H. G. Khorana, and K. J. Rothschild. 1988. Vibrational spectroscopy of bacteriorhodopsin mutants: light-driven proton transport involves protonation changes of aspartic acid residues 85, 96, and 212. *Biochemistry.* 27:8516–8520.

Brown, L. S., J. Sasaki, H. Kandori, A. Maeda, R. Needleman, and J. K. Lanyi. 1995. Glutamic acid 204 is the terminal proton release group at the extracellular surface of bacteriorhodopsin. *J. Biol. Chem.* 270: 27122–27126.

de Groot, H. J. M., G. S. Harbison, J. Herzfeld, and R. G. Griffin. 1989. Nuclear magnetic resonance study of the Schiff base in bacteriorhodopsin: counterion effects on the ^{15}N shift anisotropy. *Biochemistry.* 28:3346–3353.

Dér, A., S. Száraz, R. Tóth-Boconádi, Z. Tokaji, L. Keszthelyi, and W. Stoecknius. 1991. Alternative translocation of protons and halide ions by bacteriorhodopsin. *Proc. Natl. Acad. Sci. USA.* 88:4751–4755.

Dioumaev, A. K., H. T. Richter, L. S. Brown, M. Tanio, S. Tuzi, H. Saitô, Y. Kimura, R. Needleman, and J. K. Lanyi. 1998. Existence of a proton transfer chain in bacteriorhodopsin: participation of Glu-194 in the release of protons to the extracellular surface. *Biochemistry.* 37: 2496–2506.

Essen, L. O., R. Siegert, W. D. Lehmann, and D. Oesterhelt. 1998. Lipid patches in membrane protein oligomers: crystal structure of the bacteriorhodopsin-lipid complex. *Proc. Natl. Acad. Sci. USA.* 95: 11673–11678.

Govindjee, R., S. Misra, S. P. Balashov, T. G. Ebrey, R. K. Crouch, and D. R. Menick. 1996. Arginine-82 regulates the pK_a of the group responsible for the light-driven proton release in bacteriorhodopsin. *Biophys. J.* 71:1011–1023.

Grigorieff, N., T. A. Ceska, K. H. Downing, J. M. Baldwin, and R. Henderson. 1996. Electron-crystallographic refinement of the structure of bacteriorhodopsin. *J. Mol. Biol.* 259:393–421.

Henderson, R., J. M. Baldwin, T. A. Ceska, F. Zemlin, E. Beckmann, and K. H. Downing. 1990. Model for the structure of bacteriorhodopsin based on high-resolution electron cryo-microscopy. *J. Mol. Biol.* 213: 899–929.

Kalaidzidis, I. V., I. N. Belevich, and A. D. Kaulen. 1998. Photovoltage evidence that Glu-204 is the intermediate proton donor rather than the terminal proton release group in bacteriorhodopsin. *FEBS Lett.* 434: 197–200.

Kataoka, M., K. Mihara, H. Kamikubo, R. Needleman, J. K. Lanyi, and F. Tokunaga. 1993. Trimeric mutant bacteriorhodopsin, D85N, shows a monophasic CD spectrum. *FEBS Lett.* 333:111–113.

Kimura, Y., D. G. Vassylyev, A. Miyazawa, A. Kidera, M. Matsushima, K. Mitsuoka, K. Murata, T. Hirai, and Y. Fujiyoshi. 1997. Surface of bacteriorhodopsin revealed by high-resolution electron crystallography. *Nature.* 389:206–211.

Lanyi, J. K. 1993. Proton translocation mechanism and energetics in the light-driven pump bacteriorhodopsin. *Biochim. Biophys. Acta.* 1183: 241–246.

Luecke, H., H.-T. Richter, and J. K. Lanyi. 1998. Proton transfer pathways in bacteriorhodopsin at 2.3 angstrom resolution. *Science.* 280: 1934–1937.

Mathies, R. A., S. W. Lin, J. B. Ames, and W. T. Pollard. 1991. From femtoseconds to biology: mechanism of bacteriorhodopsin's light-driven proton pump. *Annu. Rev. Biophys. Chem.* 20:491–518.

Mehring, M. 1983. Principle of High Resolution NMR in Solids, 2nd Ed. Springer Verlag, New York.

Oesterhelt, D., and W. Stoeckenius. 1974. Isolation of the cell membrane of *Halobacterium halobium* and its fractionation into red and purple membrane. *Methods Enzymol.* 31:667–678.

Onishi, H., M. E. McCance, and N. E. Gibbons. 1965. A synthetic medium for extremely halophilic bacteria. *Can. J. Microbiol.* 11:365–373.

Pebay-Peyroula, E., G. Rummel, J. P. Rosenbusch, and E. M. Landau. 1997. X-ray structure of bacteriorhodopsin at 2.5 angstroms from microcrystals grown in lipidic cubic phases. *Science.* 277:1676–1681.

Petkova, A. T., J. G. Hu, M. Bizounok, M. Simpson, R. G. Griffin, and J. Herzfeld. 1999. Arginine activity in the proton-motive photocycle of bacteriorhodopsin: solid-state NMR studies of the wild-type and D85N proteins. *Biochemistry.* 38:1562–1572.

Rammelsberg, R., G. Huhn, M. Lübben, and K. Gerwert. 1998. Bacteriorhodopsin's intramolecular proton-release pathway consists of a hydrogen-bonded network. *Biochemistry.* 37:5001–5009.

Richter, H.-T., L. S. Brown, R. Needleman, and J. K. Lanyi. 1996. A linkage of the pKa's of asp-85 and glu-204 forms part of the reprotonation switch of bacteriorhodopsin. *Biochemistry.* 35:4054–4062.

Rothwell, W. P., and J. S. Waugh. 1981. Transverse relaxation of dipolar coupled spin systems under rf irradiation: detecting motions in solid. *J. Chem. Phys.* 75:2721–2732.

Saitô, H. 1986. Conformation-dependent ^{13}C chemical shifts: a new means of conformational characterization as obtained by high-resolution solid-state NMR. *Magn. Reson. Chem.* 24:835–852.

Saitô, H., and I. Ando. 1989. High-resolution solid-state NMR studies of synthetic and biological macromolecules. *Annu. Rep. NMR Spectrosc.* 21:209–290.

Saitô, H., S. Tuzi, and A. Naito. 1998. Empirical versus nonempirical evaluation of secondary structure of fibrous and membrane protein by solid-state NMR: a practical approach. *Annu. Rep. NMR Spectrosc.* 36:79–121.

Scharnagl, C., J. Hettenkofer, and S. F. Fischer. 1995. Electrostatic and conformational effects on the proton translocation steps in bacteriorhodopsin: analysis of multiple M structures. *J. Phys. Chem.* 99:7787–7800.

Stoeckenius, W., and R. A. Bogomolni. 1982. Bacteriorhodopsin and related pigments of halobacteria. *Annu. Rev. Biochem.* 52:587–616.

Tanio, M., S. Tuzi, S. Yamaguchi, H. Konishi, A. Naito, R. Needleman, J. K. Lanyi, and H. Saitô. 1998. Evidence of local conformational fluctuations and changes in bacteriorhodopsin, dependent on lipids, detergents and trimeric structure, as studied by ^{13}C NMR. *Biochim. Biophys. Acta.* 1375:84–92.

Tanio, M., S. Inoue, K. Yokota, T. Seki, S. Tuzi, R. Needleman, J. K. Lanyi, and H. Saitô. 1999. Long-distance effects of site-directed mutations on backbone conformation in bacteriorhodopsin from solid-state NMR of [$^{1}H^{13}C$]Val-labeled proteins. *Biophys. J.* 77:431–442.

Tuzi, S., A. Naito, and H. Saitô. 1993. A high-resolution solid-state ^{13}C-NMR study on [1-^{13}C]Ala and [3-^{13}C]Ala and [1-^{13}C]Leu and Val-labelled bacteriorhodopsin. *Eur. J. Biochem.* 218:837–844.

Tuzi, S., A. Naito, and H. Saitô. 1994. ^{13}C NMR study on conformation and dynamics of the transmembrane α-helices, loops, and C-terminus of [3-^{13}C]Ala-labeled bacteriorhodopsin. *Biochemistry.* 33:15046–15052.

Tuzi, S., A. Naito, and H. Saitô. 1996a. Temperature-dependent conformational change of bacteriorhodopsin as studied by solid-state ^{13}C NMR. *Eur. J. Biochem.* 239:294–301.

Tuzi, S., S. Yamaguchi, A. Naito, R. Needleman, J. K. Lanyi, and H. Saitô. 1996b. Conformation and dynamics of [3-^{13}C]Ala-labeled bacteriorhodopsin and bacterioopsin, induced by interaction with retinal and its analogs, as studied by ^{13}C nuclear magnetic resonance. *Biochemistry.* 35:7520–7527.

Tuzi, S., S. Yamaguchi, M. Tanio, H. Konishi, S. Inoue, A. Naito, R. Needleman, J. K. Lanyi, and H. Saitô. 1999. Location of a cation binding site in the loop between helices F and G of bacteriorhodopsin, as studied by ^{13}C NMR. *Biophys. J.* 76:1523–1531.

Xu, D., M. Sheves, and K. Schulten. 1995. Molecular dynamics study of M_{412} intermediate of bacteriorhodopsin. *Biophys. J.* 69:2745–2760.

Yamaguchi, S., S. Tuzi, T. Seki, M. Tanio, R. Needleman, J. K. Lanyi, A. Naito, and H. Saitô. 1998. Stability of the C-terminal α-helical domain of bacteriorhodopsin that protrudes from the membrane surface, as studied by high-resolution solid-state ^{13}C NMR. *J. Biochem. (Tokyo).* 123:78–86.

Zhou, F., A. Windemuth, and K. Schulten. 1993. Molecular dynamics study of the proton pump cycle of bacteriorhodopsin. *Biochemistry.* 32:2291–2306.